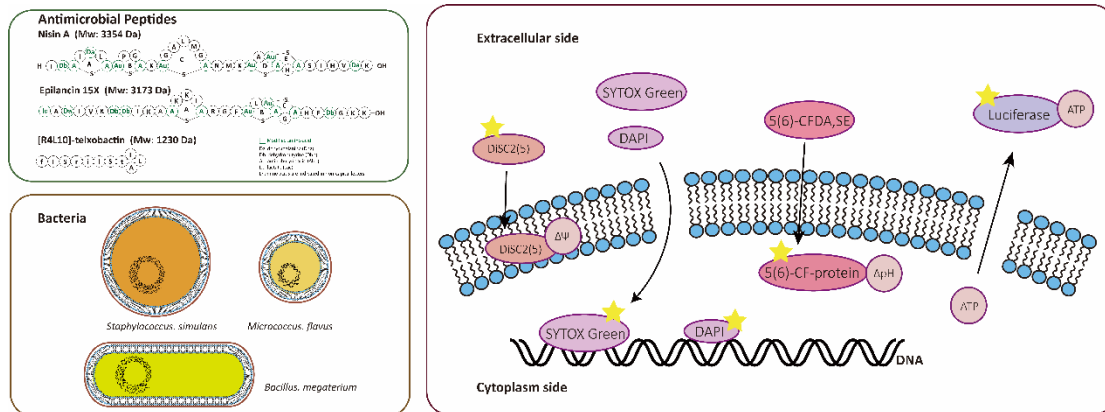


1 **Analyzing mechanisms of action of antimicrobial peptides on bacterial membranes**  
2 **requires multiple complimentary assays and different bacterial strains**



3  
4

5 Xiaoqi Wang<sup>1</sup>, Roy A. M. van Beekveld<sup>1</sup>, Yang Xu<sup>1</sup>, Anish Parmar<sup>3,4</sup>, Sanjit Das<sup>3,4</sup>,  
6 Ishwar Singh<sup>3,4</sup>, Eefjan Breukink<sup>1,2</sup>,

7

8 <sup>1</sup> Membrane Biochemistry and Biophysics, Department of Chemistry, Faculty of  
9 Science, Utrecht University, Utrecht, Netherlands.

10 <sup>2</sup> Zhejiang Provincial Key Laboratory of Food Microbiotechnology Research of China,  
11 the Zhejiang Gongshang University of China, Hangzhou, China

12 <sup>3</sup> Antimicrobial Pharmacodynamics and Therapeutics, Department of Pharmacology  
13 and Therapeutics, Institute of Systems, Molecular & Integrative Biology University of  
14 Liverpool, William Henry Duncan Building, 6 West Derby St Liverpool, L7 8TX, UK.

15 <sup>4</sup> Antimicrobial Drug Discovery and Development, Department of Chemistry, The  
16 Robert Robinson Laboratories, University of Liverpool, L69 3BX, Liverpool, UK

17 .

18 **Corresponding Author:**

19 *Dr. Eefjan Breukink*

20 *Membrane Biochemistry and Biophysics*

21 *Z807, Padualaan 8, 3584 CH, Utrecht, Netherlands*

22 *Tel: +31-(0)30 253 3523*

23 *Email: e.j.breukink@uu.nl*

24

25 **Key words:**

26 Antimicrobial peptides

27 Membrane effects

28 Membrane potential

29 pH homeostasis

30 ATP homeostasis

31

32 **Highlights:**

33 1. Using multiple assays and bacterial strains we show interrelationships between  
34 effects of several AMPs on  $\Delta\text{pH}$ , membrane potential and ATP-synthesis.

35 2. A novel assay has been developed that allows simultaneous detection of ATP

1 leakage from bacterial cells as well as drop of intracellular ATP-levels.  
2 3. This work shows that it is important to use multiple different bacteria and assays  
3 capable of measuring all aspects of membrane permeabilization when studying  
4 modes of action of AMPs.

## 5 6 **Abstract**

7 Antimicrobial peptides (AMPs) commonly target bacterial membranes and show  
8 broad-spectrum activity against microorganisms. In this research we used three  
9 AMPs (nisin, epilancin 15X, [R4L10]-teixobactin) and tested their membrane effects  
10 toward three strains (*Staphylococcus simulans*, *Micrococcus flavus*, *Bacillus*  
11 *megaterium*) in relation with their antibacterial activity. We describe fluorescence  
12 and luminescence-based assays to measure effects on membrane potential,  
13 intracellular pH, membrane permeabilization and intracellular ATP levels. The results  
14 show that our control peptide, nisin, performed mostly as expected in view of its  
15 targeted pore-forming activity, with fast killing kinetics that coincided with severe  
16 membrane permeabilization in all three strains. However, the mechanisms of action  
17 of both Epilancin 15X as well as [R4L10]-teixobactin appeared to depend strongly on  
18 the bacterium tested. In certain specific combinations of assay, peptide and  
19 bacterium, deviations from the general picture were observed. This was even the  
20 case for nisin, indicating the importance of using multiple assays and bacteria for  
21 mode of action studies to be able to draw proper conclusions on the mode of action  
22 of AMPs.

## 23 24 **1. Introduction**

25 Antimicrobial resistance is becoming a global threat to human health as more and  
26 more antibiotics are losing their efficacy. Antimicrobial peptides (AMPs) showing  
27 broad-spectrum activity against microorganisms have been considered already for a  
28 long time as promising substitutions for these antibiotics [1-3]. AMPs are mostly  
29 positively charged and amphiphilic, properties that are essential for their (initial)  
30 interaction with the negatively charged membranes of target bacteria [4]. Currently,  
31 there are three main models that are describing the possible mechanisms of action  
32 of AMPs, i.e., the barrel-stave model, carpet model and toroidal-pore model [4-6].  
33 However, these three classic models cannot account for the modes of action of many  
34 AMPs. In addition, mechanisms of actions are often ascribed to peptides while using  
35 improper model systems (e.g. composed of only one lipid) [6, 7]. Increasingly more  
36 models have been proposed by which AMPs destabilize the target membrane.  
37 Examples of these are thinning of the membrane, clustering of anionic lipids or  
38 non-lytic membrane depolarization [8-11]. Alternatively, the AMPs induce phase  
39 separations that lead to destabilization of the bacterial membranes via blebbing,  
40 budding, or vascularization [12-15]. Recently, it was shown that many AMPs lacked a  
41 correlation between membrane permeabilization and antibiotic activity. This led to  
42 the suggestion that these AMPs inhibit bacteria by perturbing the membrane and  
43 causing intracellular biomass aggregation [16]. What all AMPs have in common is  
44 their affinity for the bacterial membrane, and even those that have internal targets

1 but do not cause permeabilization have mechanisms to pass this membrane that are  
2 similar to certain pore-forming mechanisms [16]. Importantly, what mechanism a  
3 peptide is proposed to follow largely depends on the method and bacterium used for  
4 determining the peptide's effects [17, 18]. Thus, the way in which membrane  
5 permeabilization by an AMP is determined has major implications for the  
6 conclusions that can (and will) be drawn on the proposed mechanism.

7 AMPs' effects on bacterial membranes can be subtle, such as membrane  
8 depolarization or more severe, like pore-formation or disruption via the carpet  
9 model and several methods exist that can measure these effects on membranes.  
10 Dissipation of the membrane potential ( $\Delta\psi$ ) and/or  $\Delta\text{pH}$ , are the subtlest indications  
11 of membrane perturbation that can be measured. Both constitute the so-called  
12 proton-motive force (PMF,  $\Delta p$ ) where  $\Delta p = \Delta\psi - 2.3RT/F \cdot \Delta\text{pH}$  [19]. The dissipation of  
13 the PMF is triggered by proton leakage or membrane potential depolarization (ion  
14 leakage, in case of bacteria mostly  $\text{K}^+$ ). The depolarization of the membrane can be  
15 measured by voltage-sensitive cyanine dyes such as 3,3'-Diethylthiadicarbocyanine  
16 ( $\text{DiSC}_2(5)$ ) [20-23]. In the presence of a membrane potential, these dyes are absorbed  
17 into the bilayer and accumulate presumably in the inner leaflet of the plasma  
18 membrane resulting in self-quenching [24]. The dyes are released after  
19 depolarization of the membrane and as a result the self-quenching is relieved  
20 [25-27]. Changes in the pH gradient are mostly measured by determining the pH of  
21 the cytosol via internalized pH-sensitive fluorophores. Carboxyfluorescein diacetate  
22 succinimidyl ester can be used for this, where its esterized form can enter the cell and  
23 following de-esterification it becomes fluorescent [28]. The succinimidyl ester ensures  
24 stable intracellular localization. Besides dissipation of the PMF due to loss of ions or  
25 proton influx, more severe membrane damage, such as pore-formation, can be  
26 measured by determining the efflux of (much) larger intracellular components. The  
27 earliest method used for this was detecting the release of UV-absorbing components  
28 of the cell [29]. In addition, the loss of ATP by the cells can be determined by a  
29 luciferase based assay [30]. An alternative way to determine the membrane damage  
30 is using probes that can enter the cells when their membrane is damaged.  
31 DNA-binding probes such as SYTOX green or 4',6-diamidino-2-phenylindole (DAPI)  
32 are membrane impermeable and they stain the DNA only when the membrane  
33 barrier is compromised [31-38].

34 Members of the family of lantibiotics, which belongs to AMPs, usually have specific  
35 mechanisms and large amount of them indeed harbors the Lipid II targeting family  
36 members [39, 40]. Nisin (Fig. S1A) is one of the most well studied member of the  
37 lantibiotics family that targets Lipid II and forms stable pores together with Lipid II in  
38 the bacterial membrane [17, 41-43]. The A and B ring-system of nisin is responsible  
39 for binding to Lipid II and the C-terminal part of nisin including rings D/E has been  
40 suggested to be important for pore-formation [44]. A recent high-resolution NMR  
41 study revealed more details on the nisin-Lipid II binding in membrane bilayers,  
42 where the N20-K22 (the hinge) of nisin was shown to be flexible and lines the pore  
43 lumen. This was suggested to be important for the adaption of the pores to the  
44 thickness of the membrane [45]. The C-terminal (S29-K34) part of nisin was shown to

1 still be dynamic in the pore structure and it is proposed to pierce through the  
2 membrane [45]. Pores formed by nisin are very stable and black lipid bilayer studies  
3 have shown that nisin pores have a pore-size of about 2 to 2.5 nm, thus allowing  
4 molecules the size of ATP (Stokes radius of ~0.7) through the pore [43, 46]. The  
5 mode of action of epilancin 15X (Fig. S1B), another member of the lantibiotics family,  
6 is still unknown. Therefore we aimed to study the antibacterial activity of this peptide  
7 in comparison to nisin. Epilancin 15X, which has one of the lowest MICs against  
8 pathogenic bacteria and has potent activity especially against Staphylococci [47]. It is  
9 produced by *Staphylococcus epidermidis* 15X154 and was isolated and structurally  
10 characterized in 2005 [48]. The C-terminus of epilancin 15X, especially rings B and C,  
11 is very similar to nisin, which may point to pore-formation as its mechanism [47].  
12 However, epilancin 15X lacks nisin's N-terminal lipid II signature binding A/B rings  
13 system, which makes it uncertain if it interacts with Lipid II. As mentioned, how  
14 epilancin 15X acts is still unclear, but given the similarity of the C-terminal  
15 lanthionine rings it may, like nisin, attack bacteria via membrane permeabilization.  
16 Teixobactin, which is produced by *Eleftheria terrae*, kills pathogens via targeting Lipid  
17 II and the wall teichoic acid precursor Lipid III, thus its mode of action includes  
18 inhibition of the bacterial cell wall synthesis machinery [49]. Recently it was shown  
19 that teixobactin has a dual mode of action that besides cell wall synthesis inhibition  
20 also includes membrane disruption via fibril formation together with Lipid II on the  
21 membrane surface [50]. This aggregational behavior with Lipid II had been shown  
22 before for an improved teixobactin analogue, D-Arg4-Leu10-teixobactin  
23 ([R4L10]-teixobactin, Fig. S1C) [51, 52]. Hence, we also explored the permeabilization  
24 activity of this teixobactin analogue compared to that of nisin and epilancin 15X.  
25 During our efforts in studying the membrane effects of these AMPs we noticed that  
26 even a well-known pore-former, the lantibiotic nisin, sometimes behaved differently  
27 from what can be expected from a pore-forming peptide in different methods and  
28 bacteria. Our results indicate that it is important to use multiple assays and bacteria  
29 for mode of action studies to be able to draw proper conclusions on the mode of  
30 action of AMPs.

## 31 **2. Method and materials**

### 32 **2.1 Materials and strains**

33 Nisin A, epilancin 15X were prepared as previously described [48, 53].  
34 [R4L10]-teixobactin was obtained from Ishwar Singh (University of Liverpool).  
35 3,3'-Diethylthiadicarbocyanine iodide (DiSC<sub>2</sub>(5)), 4',6-diamidino-2-phenylindole  
36 (DAPI) and Triton X-100 were purchased from Sigma-Aldrich. SYTOX™ Green Nucleic  
37 Acid Stain (SYTOX green) and 5(6)-CFDA, SE, Luria Broth (LB) and Tryptone Soya  
38 Broth (TSB) were purchased from ThermoFisher. M9 medium supplemented with  
39 vitamins and salts was prepared as described [54]. BacTiter-Glo™ Microbial Cell  
40 Viability Assay Kit was purchased from Promega. All other chemicals or reagents  
41 used were of analytical grade. Strains used in this study: *S. simulans* 22 [55]; *M.*  
42 *flavus* DSM 1790; *B. megaterium* ATCC 14581.

43

### 44 **2.2 Methods**

### 1 **2.2.1 General procedures**

2 Precultures of the indicator strains were grown at 37 °C in TSB for *S. simulans* and *M.*  
3 *flavus* or LB for *B. megaterium* while shaking at 200 rpm overnight and then diluted  
4 to an OD<sub>600</sub> of 0.05 with fresh medium. The cultures were further grown for 4 hours  
5 and spun down at 3000 × g for 10 min at 4 °C. The cells were washed twice with  
6 buffer A (250 mM glucose, 5 mM MgSO<sub>4</sub>, 100 mM KCl, 10 mM potassium-phosphate  
7 buffer at pH 7) for *S. simulans* and *M. flavus* or M9 medium for *B. megaterium*. They  
8 were then resuspended to an OD<sub>600</sub> of 5 and kept on ice until use on the same day.  
9 The bacteria remained viable under these conditions for at least 2 hours.

10 The concentration of peptides was determined using the Pierce™ BCA Protein Assay  
11 Kit (Thermo Fisher) using BSA as a standard. Fluorescence and luminescence related  
12 experiments (membrane potential depolarization assay, membrane permeability  
13 assay, ATP leakage assay, proton permeability assay) were performed using a Cary  
14 Eclipse fluorescence spectrophotometer (FL0904M005) in a 10 x 4-mm quartz  
15 cuvette at 25 °C.

16 To determine the number of surviving cells in the fluorescence cuvette at a given  
17 time, 5 µL of the suspension was plated onto TSB agar plates and incubated at 37 °C  
18 overnight.

19 Per species of bacteria all the experiments were done on the same day and due to  
20 time restraints, per experiment, one set of data could only be obtained. For each  
21 bacterium this was repeated at least twice, thus generating fully independent  
22 measurements.

### 23 **2.2.2 MIC determination**

24 The concentrations of AMPs (nisin, epilancin 15X and teixobactin) that did not allow  
25 growth of the indicator strains after 18 hours were defined as the MICs. This was  
26 determined using 1 mL cultures of indicator strains at a start OD<sub>600</sub> of 0.05 in fresh  
27 medium (TSB for *S. simulans* and *M. flavus* or LB for *B. megaterium*) containing a  
28 serial dilution of antibiotics in sterilized glass tubes. The tubes were shaken at 37 °C,  
29 200 rpm and the OD<sub>600</sub> was determined after incubation for 18 hours on a Novaspec  
30 II. MIC determination were repeated three times.

### 31 **2.2.3 Membrane potential depolarization assay**

32 The fluorescent dye DiSC<sub>2</sub>(5) (excitation at 650 nm and emission at 670 nm) was  
33 used to test the effect of the antibiotics on the membrane potential of the bacteria.  
34 From the concentrated cell suspension, cells were diluted to OD<sub>600</sub>=0.05 in a cuvette  
35 containing 1 ml of buffer A, followed by the addition of 2 µL of a stock solution of 0.1  
36 mM DiSC<sub>2</sub>(5) dissolved in DMSO. Antibiotics were added after 1 minute, or left out  
37 for the blank. At the end of the experiment 10 µL of 20% Triton X-100 was added to  
38 fully dissipate the membrane potential.  
39

### 40 **2.2.4 Membrane permeability assay (DNA binding stain)**

41 The fluorescent dyes SYTOX green (excitation at 504 nm and emission at 523 nm)  
42 and DAPI (excitation at 364 nm and emission at 454 nm) were used to inspect the  
43  
44

1 abilities of the antibiotics to disrupt the bacterial membrane. From the concentrated  
2 cell suspension 10  $\mu$ L was added into a cuvette containing 1 mL buffer A to reach an  
3  $OD_{600}$  of 0.05, followed by the addition of 1  $\mu$ L of a stock solution of 0.25  $\mu$ M SYTOX  
4 green dissolved in DMSO or 1  $\mu$ L of a stock solution of 1 mg/mL DAPI dissolved in 10  
5 mM PBS at pH 7. Antibiotics were added after 1 minute, or left out for the blank. At  
6 the end of the experiment 10  $\mu$ L of 20% Triton X-100 for SYTOX green or  
7 BacTiter-Glo™ disruption buffer for DAPI was added to fully disrupt the cells.

### 8 9 **2.2.5 ATP leakage assay**

10 The BacTiter-Glo™ Microbial Cell Viability Assay Kit was used to inspect the abilities  
11 of the antibiotics to cause ATP leakage from the bacteria. Luciferase signal was  
12 recorded using the Bio/Chemi-luminescence mode with the emission set at 556 nm.  
13 The BacTiter-Glo™ substrate stock solution containing the luciferase enzyme and  
14 substrate was made by dissolving the lyophilized substrate/enzyme mixture provided  
15 in the kit in 1 mL of buffer A, which was then divided into 50  $\mu$ L aliquots and stored  
16 at -80 °C until use. From the concentrated cell suspension 10  $\mu$ L was added into a  
17 cuvette containing 1 mL buffer A, followed by the addition of 5  $\mu$ L of BacTiter-Glo™  
18 substrate solution. Antibiotics were added after 1 minute, or left out for the blank.  
19 At the end of the experiment 10  $\mu$ L of BacTiter-Glo™ disruption buffer was added to  
20 measure the amount of residual ATP that was left inside the cells. Experiments using  
21 *B. megaterium* were performed in M9 medium to maintain viability of the cells.  
22 Unfortunately, ATP measurements were incompatible with M9 medium.

### 23 24 **2.2.6 Proton permeability assay**

25 The 5(6)-CFDA, SE (excitation at 490 nm and emission at 525 nm) was used to inspect  
26 the proton permeabilities of the antibiotics against the bacteria. Precultures of  
27 indicator strains were grown at 37 °C, 200 rpm overnight, and then diluted to an  
28  $OD_{600}$  of 0.05 with fresh medium. The culture was further grown for 4 hours and  
29 spun down at 3000  $\times$  g for 10 min at 4 °C. Then cells were resuspended in buffer B  
30 containing 50 mM HEPES, 20 mM glucose, 1 mM  $MgSO_4$  at pH 7 to an  $OD_{600}$  of 0.5  
31 and incubated with 3  $\mu$ M 5(6)-CFDA, SE for 30 min at 30 °C, 200 rpm. The cells were  
32 washed twice with the same buffer and were resuspended to an  $OD_{600}$  of 5. From  
33 this cell suspension 10  $\mu$ L was added into a cuvette containing 1 mL buffer B set at  
34 pH 5. Antibiotics were added after 30 seconds, or left out for the blank. At the end of  
35 the experiment 20  $\mu$ L of a 1 mg/mL carbonyl cyanide m-chlorophenyl hydrazone  
36 (CCCP) solution in DMSO was added to fully dissipate the  $\Delta$ pH of the bacteria.

### 37 38 **2.2.7 Analysis of lipid compositions of bacteria**

39 Bacteria were grown overnight at 37°C while shaking @200 rpm in TSB in the case of  
40 *S. simulans*, or at 30°C while shaking at 200 RPM for *B. megaterium* (in LB) and *M.*  
41 *flavus* (in TSB). The overnight culture was diluted to an  $OD_{600}$  of 0.05 in 10 mL and  
42 grown to mid-log phase ( $OD_{600}$  = 0.3 - 0.4) at the same conditions as for the  
43 overnight growth. Bacteria were harvested, resuspended in 0.8 mL  $H_2O$ , after which  
44 2 mL MeOH and 1 mL  $CHCl_3$  were added and the samples were vortexed extensively.

1 Subsequently, 1 mL of CHCl<sub>3</sub> and H<sub>2</sub>O were added, the sample vortexed and then  
2 centrifuged at 1,000×g for 2 min. The organic layer (bottom) was dried under a N<sub>2</sub>  
3 stream at 40°C. The dried lipids were weighed and redissolved in 250 μL 2:1  
4 CHCl<sub>3</sub>:MeOH. Lipids were then spotted onto a NP-TLC (HPTLC-Fertigplatten  
5 Nano-ADAMANT®) at 20 μg total lipids per lane using a Camag Linomat 5. The TLC  
6 was developed in 48:48:3:1, CHCl<sub>3</sub>:EtOH:NH<sub>3</sub>:H<sub>2</sub>O with 0.2 g/L NH<sub>4</sub>Ac, dried under  
7 vacuum and then stained with iodine prior to imaging. Phospholipid species were  
8 assigned based on pure references and the bacterial lipid extracts were analyzed as  
9 three independent cultures per species.

10 For analysis of the acyl chain compositions, approximately 1 mg of the bacterial  
11 extracts were redissolved in 1 mL n-hexane. Subsequently, 200 μL MeOH containing  
12 100 g/L KOH was added and the samples were extensively vortexed for 1 min to  
13 obtain fatty acid methyl esters (FAMES). The n-hexane layer was taken, dried under a  
14 N<sub>2</sub>-stream and redissolved in 50 μL n-hexane. The FAMES were then analyzed using  
15 gas chromatography with flame-ionization detection on a Trace GC Ultra (Thermo  
16 Fisher Scientific) equipped with a biscyanopropyl polysiloxane column (Restek) and  
17 N<sub>2</sub> as a carrier gas. A temperature gradient was used that started at 40°C and held  
18 for one minute, followed by a linear gradient to 160°C in 4 min and a subsequent  
19 linear gradient to 220°C in 15 min. Peak identification was performed using FAME  
20 standards Mixture BR2 (Larodan; 90-1052) for branched species and certain straight  
21 chain fatty acids or 63-B (Nu-Chek-Prep) for various unsaturated and straight chain  
22 fatty acid species.

### 23 **3. Results**

24 The peptides under study here are targeted. Hence, to ensure that unspecific  
25 (non-targeted) mechanisms do not play a role we deliberately selected strains with  
26 low MICs to avoid clouding the results with a-specific effects.

#### 28 ***3.1 Nisin causes severe membrane disruption in S. simulans and B. megaterium 29 typical for pore-formation.***

30 Nisin displayed MIC values equal to 80 nM, 50 nM and 75 nM toward *S. simulans*, *M.*  
31 *flavus* and *B. Megaterium* respectively. In general, severe membrane disruption, e.g.  
32 pore-formation, of a bacterium leads to rapid death. This fast-killing rate should also  
33 correspond to the effects observed in the assays that are employed to determine  
34 membrane effects of AMPs if their mode of action involves membrane disruption.  
35 Therefore, we also determined the number of cells killed by nisin by determining the  
36 amount of colony forming units (CFU) after 5 minutes incubation, the average time  
37 needed for the assays employed here, at the different concentrations mentioned  
38 above. To exclude any environmental influence on the results we determined the  
39 CFUs that are present in the same cuvette and under the identical conditions used  
40 for the fluorescence experiments. From these plate assays it becomes clear that nisin  
41 is able to kill rapidly, as can be expected from its targeted pore-forming mechanism.  
42 At 5X and 10X MIC there is about a 3 and 4 log reduction respectively in viable cells  
43 after 5 minutes and after 1 minute already more than 99% of the bacteria have been  
44 killed (Fig. P1). At lower nisin concentrations (1X and 2X MIC) only a 1 or 2 log

1 reduction was achieved in 5 minutes and killing clearly takes longer.  
2 The activity of AMPs, expressed in their MIC-values, towards different strains and in  
3 comparison to others can vary quite extensively from nanomolar to micromolar  
4 values depending on the killing mechanism they use. Therefore, in order to allow  
5 easy comparison, we used AMP-concentrations equal to 1X, 2X, 5X and 10X the  
6 respective MICs of the different strains in all the assays that report on membrane  
7 effects by the AMPs.  
8 When testing the effects of nisin on the membrane potential with the dye DiSC<sub>2</sub>(5) or  
9 the effect on membrane permeability to a DNA probe with the dye Sytox  
10 green/DAPI, in all cases, a picture emerges where the membrane effects parallel the  
11 killing rates (Fig. 1A, B and S2A). At low MICs relative minor effects can be seen,  
12 while at the highest concentrations (5X and 10X MIC) the effects are maximal of  
13 what can be achieved in the assay. The ΔpH measurements deviate from this picture  
14 where already a maximum effect was achieved with a concentration of only 1X MIC  
15 in about 1 minute (Fig. 1C). An interesting case is presented when we tested for ATP  
16 leakage in an on-line assay using luciferase to determine both intra cellular ATP  
17 levels as well as ATP-leakage from the cells. As luciferase is unable to enter the cell  
18 spontaneously and is too large to leak through the pores formed by nisin, this assay  
19 allowed us to determine i) the extent of ATP leakage from the bacteria in time and ii)  
20 the total amount of ATP remaining in the bacteria after 5 minutes of incubation with  
21 nisin. The low MIC traces (1X and 2X MIC) are especially interesting as it shows that  
22 two simultaneously occurring processes have to be considered (Fig. 1D). The  
23 addition on nisin at this concentration clearly induced some leakage of ATP in 5  
24 minutes, amounting to a little over 10 % of the original amount of ATP in the cells (as  
25 deduced from the maximal signal obtained from the blank after lysis of the cells).  
26 However, simultaneously the total amount of ATP present in the cells had dropped  
27 considerable. Only about 50% of the ATP was left with respect to the control,  
28 meaning that an additional 40% of ATP was lost somehow. This drop in cellular ATP  
29 can be explained by taking into account that, within 1 minute, nisin induced a  
30 complete dissipation of the ΔpH, the main driving force for the generation of ATP in  
31 the bacteria [56]. As all ATP-consuming processes (e.g. protein synthesis, a major  
32 ATP-consumer) within the cell are still active, this results in a dramatic drop of the  
33 ATP-levels. At the highest concentration of nisin a little over 20% of the original  
34 amount of ATP has leaked out of the cells in five minutes, while nothing remains as  
35 there is no extra increase of signal upon complete lysis of the cells. Thus the  
36 remaining cells are completely devoid of ATP and have lost their ATP due to the  
37 combined losses due to leakage and consumption in the absence of ATP  
38 regeneration. So far, studies on luciferase-based ATP determination for cells have  
39 been off-line-and only determined the amount of ATP that leaked out after  
40 separating the cells from the medium. Our method is able to determine both the  
41 amount of ATP leakage in time and the total amount of ATP that is left in the cells at  
42 a given timepoint, a valuable improvement of the assay.  
43 We next tested nisin's activity towards *B. megaterium*, a bacterium with a similar  
44 sensitivity towards nisin as *S. simulans* (both 75 nM). Surprisingly, *B. megaterium*



1 seemed to be much more sensitive in the membrane disruption assays (even in M9  
2 medium) as its MIC would suggest. Membrane effects could be observed in all assays  
3 at concentrations starting 100-fold lower than the MIC, which also correlated with a  
4 rapid drop in CFUs at similar concentrations (Fig. P2). Apparently, this bacterium is  
5 much more sensitive towards nisin under the conditions of the membrane  
6 permeability tests (M9 medium) opposed to MIC tests in growth medium (LB-broth).  
7 Yet, at these lower concentrations, a fairly similar behavior of nisin was seen towards  
8 *B. megaterium* as compared to *S. simulans* with all membrane disruption assays (Fig.  
9 S2E-H). Here, the disruption of the  $\Delta\text{pH}$  was very fast as well and already complete  
10 within a minute, but also the membrane-potential measurements showed fast  
11 dissipation kinetics. Thus, both the two components of the PMF,  $\Delta\Psi$  and  $\Delta\text{pH}$ , were  
12 affected early as compared to the more severe membrane effects measured by the  
13 DNA probes. Taken together, the results with these two bacteria show that there is a  
14 good correlation between the killing rates observed and the membrane disruption  
15 measured by the different assays<sup>1</sup>.

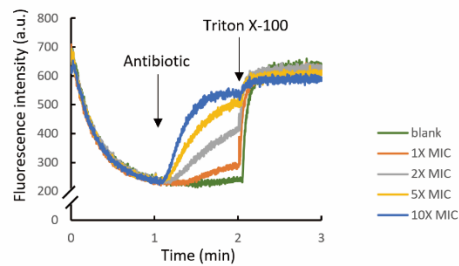
16

### 17 **3.2 Deviations from ideal behavior as a pore-former with *M. flavus***

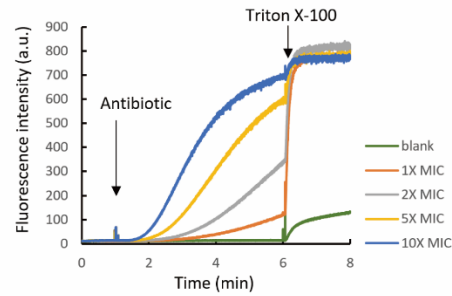
18 *M. flavus* is a bit more sensitive to nisin (MIC of 50 nM) as compared to *S. simulans*  
19 (75 nM). The killing rate of nisin towards this bacterium is similarly fast as compared  
20 to *S. simulans* as at a 10-fold MIC concentration of nisin 3-4 log killing was achieved  
21 in 5 minutes (Fig. P3).

22 The effects of nisin in the membrane potential assay, Sytox green assay and  
23 ATP-leakage assay on *M. flavus*, were all comparable to the effects observed for the  
24 other bacteria (Fig. S2B-C and Fig. 1F). Surprisingly, the effects of nisin on the  $\Delta\text{pH}$  of  
25 *M. flavus* was much less pronounced. Instead of a rapid decrease of the signal in the  
26 first minutes as seen for the other bacteria, a gradual decrease over time was  
27 observed (Fig. 1E). This coincided with a low drop of ATP levels within the cells at the  
28 lower concentrations, again showing that the  $\Delta\text{pH}$  and the ATP content of the cells  
29 are correlated. Importantly, the leakage assay using DAPI was completely  
30 non-responsive to the effects of nisin on *M. flavus* (Fig. S2D). Since DAPI is a factor of  
31  $\sim 2$  times smaller than Sytox green the size of the probe cannot explain this  
32 difference in responsiveness. This deviation from the ideal behavior signifies that  
33 relying on only one bacterium and one assay for determining membrane effects can  
34 be very limiting and can lead to complete misinterpretation of the mode of action.  
35 The non-responsiveness of DAPI stands out (also for the other peptides, see below)  
36 and makes this probe unsuitable for this kind of membrane permeability assays, at  
37 least in combination with *M. flavus*.

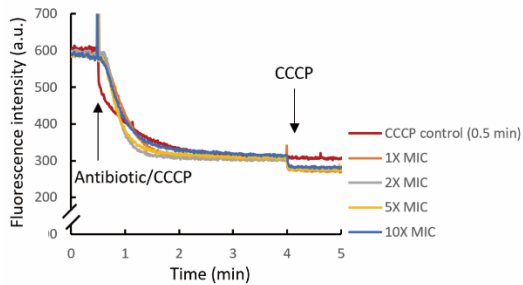
### A. *S. simulans* - $\Delta\psi$



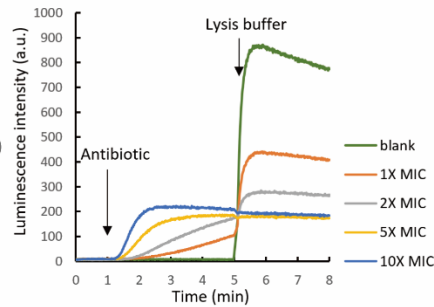
### B. *S. simulans* - permeability (Sytox green)



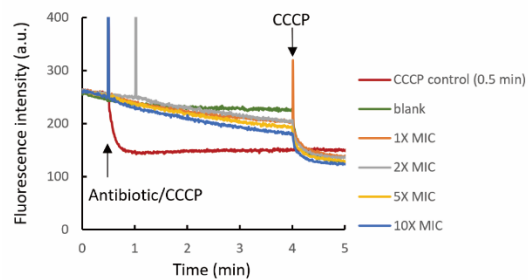
### C. *S. simulans* - $\Delta pH$



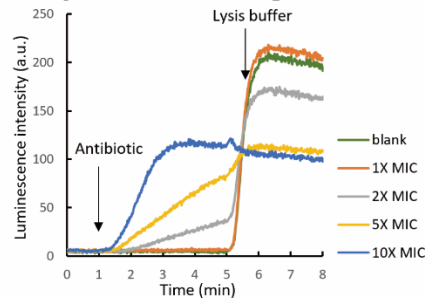
### D. *S. simulans* - ATP-leakage



### E. *M. flavus* - $\Delta pH$



### F. *M. flavus* - ATP-leakage



1

2 **Figure 1. Effects of nisin on the membranes of *S. simulans* and *M. flavus***  
3 **determined using different fluorescent probes on (A) the membrane potential of *S.***  
4 ***simulans*; (B) the membrane permeability of *S. simulans* determined using Sytox**  
5 **green; (C) the intracellular pH of *S. simulans*; (D) the in intracellular ATP levels and**  
6 **leakage of ATP from *S. simulans*; (E) the intracellular pH of *M. flavus*; (F) the**  
7 **intracellular ATP levels and leakage of ATP from *M. flavus*. The addition of samples**  
8 **(antibiotics, TritonX-100, CCCP, Lysis buffer) is indicated by arrows. Different**  
9 **amounts of nisin which were equal to 1X MIC (orange), 2X MIC (grey), 5X MIC**  
10 **(yellow) and 10X MIC (blue) are indicated by different color. Blank and CCCP**  
11 **control trace are indicated by green and red. For each bacterium this was repeated**  
12 **twice, thus generating fully independent measurements. Experiment 1E was**  
13 **repeated three times.**

14

### 15 **3.3 Epilancin 15X does not cause major membrane disruptions in *M. flavus* and *S.*** 16 ***simulans*.**

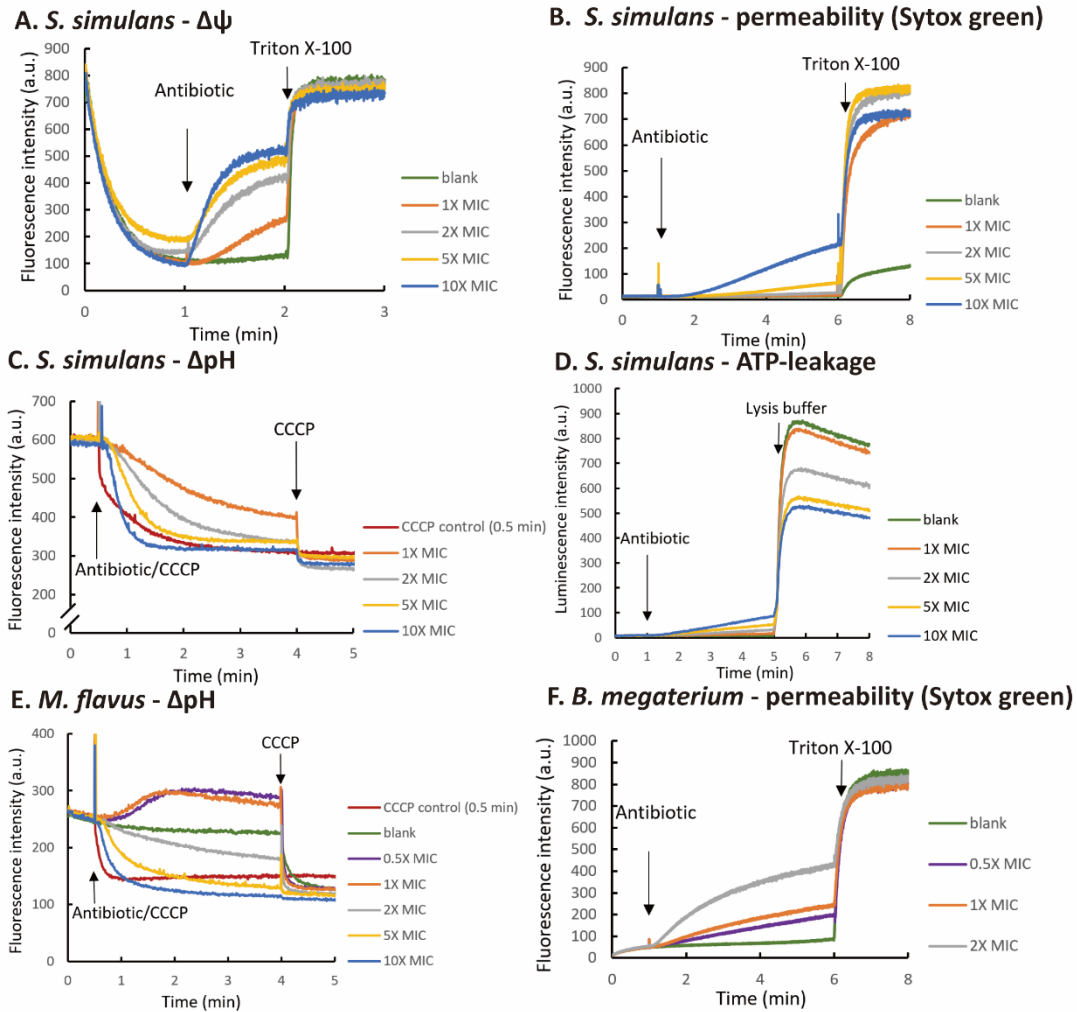
17 Epilancin 15X (abbreviated to epilancin) displayed MIC values equal to 100 nM, 75  
18 nM and 100 nM toward *S. simulans*, *M. flavus*, *B. Megaterium* respectively. Epilancin  
19 behaved quite differently from nisin towards *S. simulans* and *M. flavus*. In contrast to  
20 nisin, epilancin was shown to be bacteriostatic towards both *S. simulans* and *M.*

1 *flavus*; only 1-2 log of cells were killed at the highest concentration (10X MIC) in 5  
2 min (Fig. P4 and P5). The bacteriostatic effect of epilancin towards these strains  
3 would suggest that it has less severe membrane perturbing activity. This, we tested  
4 using the assays we have validated with nisin as a reference compound above.  
5 First, we used DiSC<sub>2</sub>(5) and 5(6)-CFDA, SE to test the membrane depolarization  
6 activity and proton permeabilization activity of epilancin toward the two strains.  
7 Epilancin causes clear effects in both assays with *S. simulans* that increase with  
8 increasing concentration (Fig. 2A and C) albeit that the effects on the  $\Delta$ pH were not  
9 as strong as those of nisin (compare Figures 1C and 2C). Interestingly, concentrations  
10 of epilancin of 0.5X MIC and 1X MIC do not appear to cause proton permeability in  
11 *M. flavus* (Fig. 2E). On the contrary, the signal has a clear increase, pointing to  
12 increased outflow protons from the cells.  
13 In line with epilancin's bacteriostatic activity, it barely shows effects on membrane  
14 permeability in experiments using Sytox green, DAPI and luciferase (Fig. 2B and D,  
15 Fig. S3A, C and E). Only at high concentrations (5x & 10X MICs) some minor effects  
16 can be seen. Furthermore, although epilancin barely causes any ATP leakage from *S.*  
17 *simulans* or *M. flavus*, it did cause the internal ATP concentration to drop in both  
18 cells at the higher concentrations (Fig. 2D and S3E) albeit not to a large extent.  
19 Previously, epilancin was predicted to kill bacteria via pore-formation in view of  
20 similarities between the structures of epilancin and nisin [47]. Our results show that  
21 this cannot be the case, at least not with respect to its activity towards *S. simulans*  
22 and *M. flavus*.

23

#### 24 **3.4 Epilancin 15X activity towards *B. megaterium***

25 Similar to what we observed for nisin, *B. megaterium* was also very sensitive to  
26 epilancin. It was clearly bactericidal as at 5X MIC it caused a 4-log reduction in cells  
27 after 5 minutes (Fig. P6). This high sensitivity was also reflected in the membrane  
28 depolarization assay, where epilancin, like nisin, showed membrane depolarization  
29 activity below its MIC value. At 0.1X MIC, epilancin exhibited already more than 50%  
30 membrane depolarization in two minutes and effects were maximal at  
31 concentrations of 1X MIC or higher (Fig. S3F). The proton permeability assay showed  
32 similar results (Fig. S3H). Moreover, the Sytox green and DAPI assays indicated  
33 severe membrane damage at these higher concentrations (Fig. 2F and S3G) and  
34 these effects parallel the killing rates. Thus, these results suggest that the  
35 bactericidal activity of epilancin towards *B. megaterium* is mainly due to its  
36 membrane damaging effect.



1  
 2 **Figure 2. Effects of epilancin 15X on the membrane of *S. simulans*, *M. flavus* and *B.***  
 3 ***megaterium* determined using different fluorescent probes on (A) the membrane**  
 4 **potential of *S. simulans*; (B) the membrane permeability of *S. simulans* determined**  
 5 **using Sytox green; (C) the intracellular pH of *S. simulans*; (D) the intracellular ATP**  
 6 **levels and leakage of ATP from *S. simulans*; (E) the intracellular pH of *M. flavus*; (F)**  
 7 **the membrane permeability of *B. megaterium* determined using Sytox green. The**  
 8 **addition of samples (antibiotics, TritonX-100, CCCP, Lysis buffer) is indicated by**  
 9 **arrows. Different amounts of epilancin 15X which were equal to 0.5X MIC (purple),**  
 10 **1X MIC (orange), 2X MIC (grey), 5XMIC (yellow) and 10X MIC (blue) are indicated**  
 11 **by different color. Blank and CCCP control trace are indicated by green and red. For**  
 12 **each bacterium this was repeated twice, thus generating fully independent**  
 13 **measurements. Experiment 2E was repeated three times.**

### 14 3.5 [R4L10]-teixobactin induced membrane permeabilization

15 [R4L10]-teixobactin displayed a MIC value of 0.125  $\mu\text{g/ml}$  (100 nM) which is 2-fold  
 16 lower MIC than that of the natural version against MRSA ATCC 33591 [52]. Besides, it  
 17 displays MICs in the range of 0.25-1  $\mu\text{g/ml}$  (200-800 nM) against VRE, 0.03-0.5  
 18  $\mu\text{g/ml}$  (24-400 nM) against MRSA, and 0.125-0.5  $\mu\text{g/ml}$  (100-400 nM) against  
 19 *Bacillus* spp. [52]. In this research, [R4L10]-teixobactin displayed MIC values equal to  
 20

1 1000 nM, 750 nM and 500 nM toward *S. simulans*, *M. flavus*, *B. Megaterium*  
2 respectively. Thus, our MIC values were close to the range of MIC-values found in  
3 the literature even though we used a different method to determine them. The MIC  
4 values of [R4L10]-teixobactin toward our three test strains are 6-10 folds higher than  
5 that of nisin and epilancin 15X, therefore, to prevent possible a-specific effects due  
6 to high peptide concentrations, we only used concentrations equal to 1X, 2X and 5X  
7 the MICs of [R4L10]-teixobactin in our membrane disruption assays.

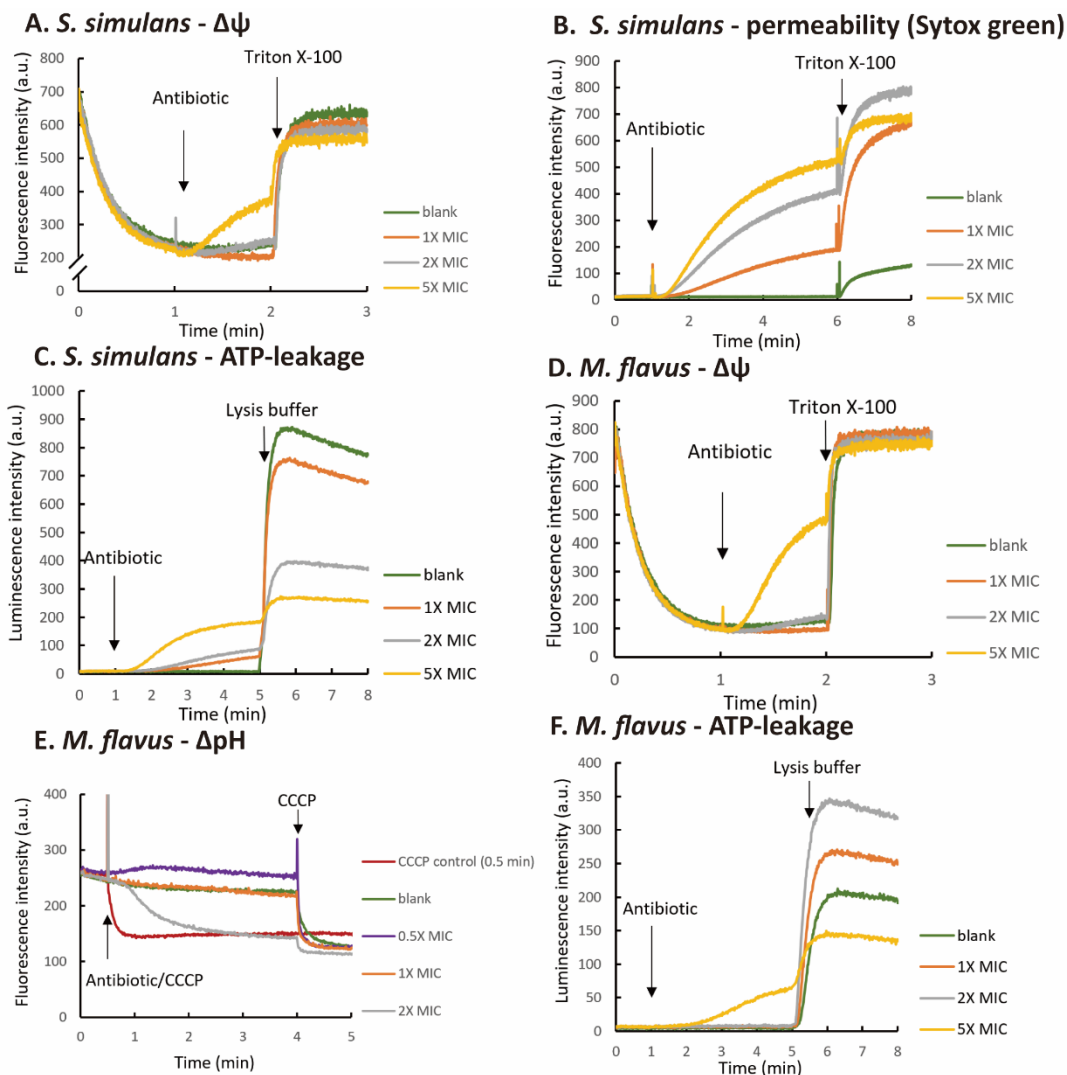
8 At lower [R4L10]-teixobactin concentrations (1X and 2X MIC), it barely killed *S.*  
9 *simulans* until at 5X MIC, the number of viable cells dropped with 90% in 5 min (Fig.  
10 P7). Similar to the case of epilancin, [R4L10]-teixobactin only showed killing activity  
11 toward *S. simulans* at the highest concentrations. The time killing assay indicated  
12 that [R4L10]-teixobactin should have a relatively low membrane perturbing activity  
13 compared to nisin, at least within the short time frame used here.

14 The membrane depolarization activity of [R4L10]-teixobactin toward *S. simulans* was  
15 in line with its low membrane-perturbing activity. Only at the highest concentration  
16 (5X MIC) a clear membrane depolarization effect could be observed and the maximal  
17 amount of dissipation that was reached in the experiment stayed below the 50%  
18 (Fig. 3A). Similarly, the  $\Delta$ pH was dissipated at concentrations higher than 1x MIC,  
19 with maximal effects only at a 5X MIC concentration (Fig. S4B). While similar results  
20 were observed in the DAPI assay (Fig. S4A), the Sytox green assay showed a different  
21 picture. A clear membrane permeability effect was observed already at 1X MIC and  
22 the maximal effect that was obtained at 5X MIC was above 70% (Fig. 3B). In line with  
23 these results, [R4L10]-teixobactin induced ATP leakage, and a low but significant  
24 amount of ATP was released from the cells at 1X MIC (Fig. 3C). Like nisin, a dual  
25 effect could be seen here as the cytosolic ATP concentration dropped significantly at  
26 concentrations equal to 2X and 5X MIC (Fig. 3C).

27 Similar to its activity towards *S. simulans*, [R4L10]-teixobactin killed 90% of *M. flavus*  
28 cells in 5 minutes at a concentration equal to 5X MIC (Fig. P8). Likewise, its effects on  
29 the membrane potential (Fig. 3D) and  $\Delta$ pH were also comparable (Fig. 3E) including  
30 the rise of the cellular pH at low concentrations of the peptide. No severe  
31 permeabilization could be observed at all concentrations in the Sytox assay and ATP  
32 only leaked out of the cells at the highest 5X MIC concentration (Fig. S4D and 3F).  
33 The DAPI results were (again) hardly showing any response with *M. flavus*, only some  
34 effect at 5X MIC could be observed (Fig. S4C). A very interesting effect could be  
35 observed for low concentrations (1 and 2X MIC) of [R4L10]-teixobactin on the  
36 internal ATP levels. A clear increase in total ATP levels of this bacterium could be  
37 observed, which we have never seen before in this test and seems unique for this  
38 combination of antibiotic and bacterial strain (Fig. 3F).

39 As observed for the other peptides, *B. megaterium* was more sensitive towards  
40 [R4L10]-teixobactin as well. More severe effects in the time-killing assay was  
41 paralleled by severe effects in the assays reporting on membrane permeabilization.  
42 [R4L10]-teixobactin at 2X MIC killed 3-log of cells in 5 min while at lower  
43 concentrations the effect was substantially lower in this time period (Fig. P9). In all  
44 membrane perturbation assays with *B. megaterium*, [R4L10]-teixobactin exhibited

1 clear effects at 0.5X MIC and reached nearly 100% at the concentration of 2X MIC  
 2 (Fig. S4E-H).



3  
 4 **Figure 3. Effects of [R4L10]-teixobactin on the membrane of *S. simulans* and *M.***  
 5 ***flavus* determined using different fluorescent probes on (A) the membrane**  
 6 **potential of *S. simulans* determined using DiSC<sub>2</sub>(5); (B) the membrane permeability**  
 7 **of *S. simulans* determined using Sytox green; (C) the ATP levels and leakage of ATP**  
 8 **from *S. simulans*; (D) the membrane potential of *M. flavus*; (E) the intracellular pH**  
 9 **of *M. flavus* determined, SE; (F) the ATP levels and leakage of ATP from *M. flavus*.**  
 10 **The addition of samples (antibiotics, TritonX-100, Lysis buffer) is indicated by**  
 11 **arrows. Different amounts of [R4L10]-teixobactin which were equal to 0.5X MIC**  
 12 **(purple), 1X MIC (orange), 2X MIC (grey) and 5X MIC (yellow) are indicated by**  
 13 **different color. Blank and CCCP control trace are indicated by green and red. For**  
 14 **each bacterium this was repeated twice, thus generating fully independent**  
 15 **measurements. Experiments 3E and 3F were repeated three times.**

16  
 17 **3.6 The ultra-sensitivity of *B. megaterium* may be related to membrane lipid**  
 18 **composition.**

19 What stood out in the experiments above was that the *B. megaterium* cells were

1 very sensitive and rapidly killed by all three antibiotic peptides. This was always  
2 paralleled by severe membrane perturbation. To test if this may be caused by the  
3 membrane lipid composition of this strain compared to the other strains we  
4 determined their composition with respect to the acyl chain and headgroup. There  
5 were some differences observed in acyl chain composition between the three strains  
6 (Fig. S5). However, these small differences do likely not explain the high sensitivity of  
7 *B. megaterium* vs the other strains. This changed when the headgroup composition  
8 was determined (Fig. S6). Phosphatidylglycerol (PG) and cardiolipin (CL) were  
9 predominantly found in *S. simulans* and *M. flavus*, while phosphatidylethanolamine  
10 (PE) could only be observed for *B. megaterium*. Most conspicuous was the absence  
11 of Lysyl-PG, a version of PG with a lysine attached making it the only known naturally  
12 occurring cationic lipid [57], in the *B. megaterium* abstract. Lysyl-PG is synthesized  
13 from PG and flopped to the outer monolayer of the plasma membrane by MprF, and  
14 is involved in resistance against positively charged AMPs [58]. *B. megatrium* lacks the  
15 gene encoding for MprF, which explains the absence of this lipid in the extracts.  
16 Therefore, it is tempting to speculate that this absence of Lysyl-PG causes *B.*  
17 *megaterium* to be highly sensitive to the membrane-disruptive effects of the AMPs  
18 from in this study.  
19

## 20 **4. Discussion**

21 Fluorescent probes that can measure, somehow, the extent of membrane damage is  
22 often used for determining the mode of action of antimicrobial peptides or other  
23 antibiotic compounds. Depending on the probe used, moderate or more severe  
24 effects on the permeability barrier of the bacterial plasma membrane are measured.  
25 Here we used five different assays and three different bacterial strains and  
26 compared how they report on the mode of action of three different antimicrobial  
27 peptides. First we tested how the different assays report on the well-established  
28 mode of action of nisin, that together with Lipid II efficiently forms pores in target  
29 membranes. Then, we tested these systems on two other peptide antibiotics. One  
30 peptide with a so far unknown mode of action was the lantibiotic epilancin 15X. The  
31 mode of action of the other, the [R4L10] analog of teixobactin, also involves  
32 targeting Lipid II and, similar to nisin, it clusters into higher order oligomers in a Lipid  
33 II dependent way. Recently, natural teixobactin was shown to induce membrane  
34 disruption in conjunction to its assembly into higher order oligomers. Whether this is  
35 also the case for the [R4L10] analog was not known [50].

### 36 **4.1 General considerations**

37 Changes in the internal pH of the cell that we measured using 5(6)-CFDA, SE or in the  
38 trans-membrane potential measured by DiSC<sub>2</sub>(5) were considered as moderate  
39 membrane permeabilization effects as they report on leakage of protons into and of  
40 (mainly) potassium ions out of the cells respectively. More severe membrane effects  
41 we determined by measuring the leakage of DNA probes into, or ATP from the cells.  
42 For the latter we devised an on-line luciferase-based assay that is able to determine  
43 both the leakage of ATP from the cells as well as the remaining ATP pool left in the

1 cytosol. The membrane potential and  $\Delta\text{pH}$  are directly linked to the cell's ability to  
2 generate ATP [56]. Thus, these three assays are, in principle, connected. The two  
3 DNA-dye based assays differ in terms of the size of the dye where SYTOX-green (MW  
4 600 g/mol) is more than twice the size of DAPI (MW 277 g/mol) and thus may report  
5 differently based on the severity of the membrane perturbation. We have no  
6 evidence of these probe interference by the peptides.

7 Data from the previous century on polymeric exclusion thresholds of Gram-positive  
8 cell walls indicated that this threshold is rather high (e.g. number average molecular  
9 weight,  $M_n=30,000$  to  $57,000$  for *B. megaterium* and  $M_n=25,000$  for *Micrococcus*  
10 *lysodeikticus*) [59]. Likely the *staphylococci* have similar thresholds. This fits nicely  
11 with more recent data on the architecture of Gram-positive cell walls of *B. subtilis*  
12 and *S. aureus* of which the smallest determined pore-size present at the inner side of  
13 the peptidoglycan layer was  $\sim 6$  nm [60]. Thus, the different dyes are not expected to  
14 be affected by different cell wall architectures. Indeed, we haven't detected any  
15 evidence for different behavior of the dyes with the different bacterial strains.

16 We consider severe membrane perturbation as the fastest way to kill bacteria and  
17 we could clearly find a good correlation between the killing kinetics of nisin and the  
18 assays that report on severe membrane disruption. An existing correlation between  
19 killing kinetics and membrane permeabilization is important to draw proper  
20 conclusions on whether the mechanism of action involves membrane perturbation.  
21 However, it should be noted that it is impossible to immediately stop the killing of  
22 bacteria by nisin (or any other AMP) while determining the number of CFUs after  
23 treatment. The amount of viable cells will likely continue to drop to some extent  
24 after plating out and incubation overnight, leading to a possible over estimation of  
25 the killing rate, especially if the AMPs have fast killing kinetics. Additionally, it should  
26 be realized that the membrane permeability experiments are only "sensitive" for up  
27 to two log reductions in cell numbers, as they cannot discriminate between 99%  
28 killing (2-log reduction) or 99.9% killing (3-log reduction). Nevertheless, whenever  
29 we noticed a higher than 2-log reduction of cell numbers after 5 minutes, this always  
30 correlated with the occurrence of severe membrane disruption in the assays. We  
31 noticed that, in general, there seemed to be a specific order in which these  
32 membrane perturbation effects are occurring. The ion and proton gradients are the  
33 first to be dissipated. Often, within the first minute after addition on the AMPs  
34 maximal effects were seen in the assays that measured the  $\Delta\text{pH}$  and  $\Delta\Psi$ , while  
35 ATP-leakage and the Sytox green signal only appeared after a lag time (usually 30  
36 seconds to 1 minute). Yet, only the Sytox, DAPI and ATP assays correlated with  
37 bacterial killing, which implies that the effect on the  $\Delta\text{pH}$  and  $\Delta\Psi$  alone, although  
38 stress related, are not sufficient to conclude that AMP's (or other compound's)  
39 killing mode involves membrane perturbation.

#### 40 **4.2 Specific observations.**

##### 41 **4.2.1 Nisin**

42 From a targeted pore-former such as nisin it is to be expected that, provided it is  
43 able to reach Lipid II in the target membrane, it will cause severe membrane  
44 disruption. The pore-size of the nisin-lipid II pore-complex, estimated to be of about



1 2 nm in diameter, would easily allow passage of ATP and the DNA probes used in this  
2 study [46]. This was indeed what we observed, as virtually all assays indicated fast  
3 and severe membrane effects. There were however two exceptions; the DAPI assay  
4 with *M. flavus* and the proton permeability assay with the same bacteria. In  
5 combination with *M. flavus*, the DAPI probe displayed strange behavior compared to  
6 Sytox green with all the peptides tested here. This suggests that this combination of  
7 probe and bacterium is for some reason not compatible, emphasizing the need for  
8 multiple probes and bacteria when testing membrane effects of AMPs and proper  
9 positive controls. Our observation that nisin didn't cause a rapid and full dissipation  
10 of the proton gradient in *M. flavus* even at very high (10 X MIC) concentrations was  
11 especially surprising in relation to the results obtained with the other probes that all  
12 show (at least some) membrane perturbation at 1-2 X MIC. The other two peptides  
13 did show dissipation of the  $\Delta$ pH, which, together with the behavior of the control  
14 (CCCP), rule out that 5(6)-CFDA is, similar to DAPI, not compatible with *M. flavus*. We  
15 currently do not have a good explanation for this aberrant effect of nisin on the pH  
16 gradient in *M. flavus*.

#### 17 18 **4.2.2 Epilancin 15X**

19 The mechanism of action of epilancin 15X appeared to be different for all the three  
20 test strains we used. It acted bactericidal towards *B. megaterium* and, in line with  
21 this, it clearly induced membrane permeabilization in all our experiments even at  
22 concentrations lower than the MIC. The clear effects in the Sytox green and DAPI  
23 assays indicate a severe membrane damaging effect in this bacterium, possibly  
24 involving pore-formation. In contrast, epilancin 15X acted bacteriostatic towards *S.*  
25 *simulans* and *M. flavus* and displayed severe membrane effects (Sytox green influx  
26 and ATP-leakage) at relative high concentrations only with *S. simulans*. While with  
27 most assays a similar activity could be observed with the two bacteria, *M. flavus*  
28 showed a surprising increase of the internal pH in the presence of low (0.5 and 1 X  
29 MIC) peptide concentrations. At these concentrations no drop in cellular ATP levels  
30 and only a small dissipation of the membrane potential could be detected. This  
31 picture suggests that epilancin 15X targets an ATP-consuming process, while also the  
32 ATP-synthesis is inhibited, which in turn decreases the influx of protons [61]. In the  
33 meantime, protons are still pumped out of the cells by the respiratory chain. These  
34 effects together led to the increase of the cellular pH [62].

35 The inhibition of ATP-synthesis is most likely the result of the epilancin-induced  
36 dissipation of the membrane potential, the main determinant of the activity of the  
37 ATP-synthase [63-65]. Because bacteria maintained a  $\Delta$ pH (which even increased at  
38 low concentrations) this suggests that the membrane is still intact. Therefore, the  
39 dissipation of the membrane potential is unlikely caused by a direct effect on the  
40 bilayer lipids of *M. flavus*, but may rather involve perturbation of the ion  
41 homeostasis in another way. A direct effect on ion transporters cannot be ruled out.

#### 42 43 **4.2.3 [R4L10]-teixobactin**

44 The binding mode of [R4L10]-teixobactin to Lipid II in bacterial membranes was

1 elucidated recently. The C-terminal depsi-cycle of teixobactin binds the  
2 pyrophosphate and MurNAc parts of Lipid II whereupon it assembles into antiparallel  
3  $\beta$ -sheets in the membrane [51]. This is followed by a slower formation of a  
4 supramolecular fibrillar structure. For natural teixobactin, this was recently also  
5 shown [50]. The multimeric structure of the natural form contains, like the [R4L10]  
6 variant a concentrated hydrophobic patch and displays curvature that results in local  
7 thinning of the membrane upon fibril formation, which was considered as the reason  
8 for teixobactin's ability to cause membrane permeabilization. The polyprenyl tails of  
9 Lipid II that are concentrated within the hydrophobic patch are proposed to also play  
10 an active role in the membrane perturbation [50]. Although the 10<sup>th</sup> amino acid  
11 *allo*-enduracididine of teixobactin is replaced by leucine in [R4L10]-teixobactin which  
12 reduces Lipid II binding affinity, the interaction of R4L10 teixobactin with Lipid II  
13 resembles that of natural teixobactin in these aspects [50, 51]. Indeed, we could  
14 show with our assays that also [R4L10]-teixobactin was able to permeabilize  
15 bacterial membranes, albeit that the severity of this permeabilization depended on  
16 the strain tested.

17 Similar as was observed for epilancin 15X, [R4L10]-teixobactin displayed different  
18 behavior towards the three different indicator strains. Towards *B. megaterium*,  
19 killing was paralleled by membrane perturbations in all assays, suggesting that  
20 membrane perturbation is a major aspect of [R4L10]-teixobactin's mechanism of  
21 action towards this bacterium. While [R4L10]-teixobactin induced somewhat less  
22 severe membrane effects towards *S. simulans*, which were in line with previous  
23 results, *M. flavus* was not that sensitive to [R4L10]-teixobactin [50]. What again  
24 stood out with this bacterium was an increased intracellular pH at 0.5 X MIC, that  
25 was also observed for epilancin, albeit that the effect was less severe with the  
26 [R4L10]-teixobactin variant. Interestingly and contrasting the effects of epilancin on  
27 this bacterium, [R4L10]-teixobactin caused an increase in intracellular ATP at the  
28 lower concentrations. This suggests that at least one major ATP-consuming  
29 biosynthesis pathway has been stopped and that the ATP-synthase remained active.  
30 Inhibition of ATP-consumption in the cells is most likely caused by blocking  
31 peptidoglycan and wall teichoic acid biosynthesis pathways via binding of the  
32 teixobactin analog to the isoprenoid-based precursors [50, 51]. The lack of effect on  
33 the membrane potential in these bacteria would explain that the ATP-synthase  
34 activity remains intact. Active ATP-synthesis would then explain the lesser effects on  
35 the internal pH at low concentrations (0.5 and 1.0 x MIC), as protons would be  
36 flowing back to the cytosol via the ATP-synthase.

37

## 38 **5. Conclusions**

39 In this research, we have developed an on-line ATP measurement which determines  
40 the extent of ATP leakage from the bacteria in time and the total amount of ATP  
41 remaining in the bacteria. The on-line ATP measurements combined with membrane  
42 potential depolarization assays and proton permeability assays reflect how  
43 antibiotics interfere with the intracellular homeostasis of the pH, ions and ATP,  
44 which are highly interconnected and regulated. These three assays combined form a

1 very powerful tool to reveal antimicrobial mechanisms. In view of their  
2 connectedness, we recommend to always combine these three assays if membrane  
3 effects of AMPs or other compounds are studied.

4 Almost all assays were consistent with the mode of action of nisin as the typical  
5 example of a targeted pore-former. Yet, even for such a clear MOA, deviations were  
6 observed in certain assay-bacterium combinations. This points to the importance of  
7 using multiple assays and bacteria for (general) mode of action studies.

8 The different behavior of epilancin 15X to the three strains makes it difficult to  
9 propose one general mode of action for this peptide. This, together with the recently  
10 found antagonization of the activity of epilancin 15X by Lipid II and, to a lesser extent,  
11 DOPG [40], indicates the need for further investigation of epilancin's mechanism of  
12 action in relation to its possible target.

13 For [R4L10]-teixobactin it is clear that its primary target, like natural teixobactin, is  
14 Lipid II and other prenyl-pyrophosphate-linked precursors [66]. The interaction with  
15 Lipid II leads to the formation of supramolecular fibrillar structures on the target  
16 membrane [50]. Whether the formation of these fibrillar structures leads to  
17 membrane damaging effects seems to depend on the membrane lipid composition  
18 of the target strain that is tested.

#### 19 **Footnotes:**

20  
21 1. Triton X-100 only induced a 100% effect in the control situation of our Sytox-green  
22 with *B. megaterium*. For the other two bacteria, a 100% effect was only obtained  
23 upon Triton X-100 addition to the cells in the presence of the peptides. Triton X-100  
24 addition did cause a 100% effect with all bacteria in the membrane depolarization  
25 assay. Another example of the higher sensitivity of this assay to relative minor  
26 membrane perturbations.

27 The lysis buffer supplied with the BacTiter-Glo kit seemed to be an efficient way for  
28 bacterial cell lysis and was compatible with the membrane depolarization, where it  
29 gave the same results, and DAPI assays. However, it was not compatible with the  
30 Sytox-green assay as this led to significant quenching of the fluorescence.

#### 31 32 **Declaration of competing interest**

33 The authors declare that they have no known competing financial interests or  
34 personal relationships that could have appeared to influence the work reported in  
35 this paper.

#### 36 37 **Acknowledgements**

38 X. Wang (201508330301) and Y. Xu (201606230222) were funded by the China  
39 Scholarship Council. I.S. acknowledges the Innovate UK and Department of Health  
40 and Social Care (DHSC), UK and Rosetrees Trust for their kind support (SBRI grant  
41 106368-623146 and Rosetrees Trust grant CF-2021-2\102). The views expressed in  
42 this publication are those of the authors and not necessarily those of Innovate UK or  
43 DHSC, UK.

44

## References

- [1] W.C. Wimley, K. Hristova, Antimicrobial peptides: successes, challenges and unanswered questions, *The Journal of membrane biology*, 239 (2011) 27-34.
- [2] K. Reddy, R. Yedery, C. Aranha, Antimicrobial peptides: premises and promises, *International journal of antimicrobial agents*, 24 (2004) 536-547.
- [3] A.R. Koczulla, R. Bals, Antimicrobial peptides, *Drugs*, 63 (2003) 389-406.
- [4] K.A. Brogden, Antimicrobial peptides: pore formers or metabolic inhibitors in bacteria?, *Nature Reviews Microbiology*, 3 (2005) 238-250.
- [5] Z. Oren, Y. Shai, Mode of action of linear amphipathic  $\alpha$ -helical antimicrobial peptides, *Peptide Science*, 47 (1998) 451-463.
- [6] H.W. Huang, F.-Y. Chen, M.-T. Lee, Molecular mechanism of peptide-induced pores in membranes, *Physical review letters*, 92 (2004) 198304.
- [7] Z. Oren, Y. Shai, Mode of action of linear amphipathic  $\alpha$ -helical antimicrobial peptides, *Peptide Science*, 47 (1998) 451-463.
- [8] K. Lohner, New strategies for novel antibiotics: peptides targeting bacterial cell membranes, *General physiology and biophysics*, 28 (2009) 105-116.
- [9] R.M. Epand, R.F. Epand, Bacterial membrane lipids in the action of antimicrobial agents, *Journal of peptide science : an official publication of the European Peptide Society*, 17 (2011) 298-305.
- [10] H.H. Haukland, H. Ulvatne, K. Sandvik, L.H. Vorland, The antimicrobial peptides lactoferricin B and magainin 2 cross over the bacterial cytoplasmic membrane and reside in the cytoplasm, *FEBS Letters*, 508 (2001) 389-393.
- [11] L.T. Nguyen, E.F. Haney, H.J. Vogel, The expanding scope of antimicrobial peptide structures and their modes of action, *Trends Biotechnol*, 29 (2011) 464-472.
- [12] D. Gidalevitz, Y. Ishitsuka, A.S. Muresan, O. Konovalov, A.J. Waring, R.I. Lehrer, K.Y. Lee, Interaction of antimicrobial peptide protegrin with biomembranes, *Proc Natl Acad Sci U S A*, 100 (2003) 6302-6307.
- [13] V.C. Kalfa, H.P. Jia, R.A. Kunkle, P.B. McCray, Jr., B.F. Tack, K.A. Brogden, Congeners of SMAP29 kill ovine pathogens and induce ultrastructural damage in bacterial cells, *Antimicrob Agents Chemother*, 45 (2001) 3256-3261.
- [14] M.E. Falagas, S.K. Kasiakou, Colistin: the revival of polymyxins for the management of multidrug-resistant gram-negative bacterial infections, *Clinical infectious diseases : an official publication of the Infectious Diseases Society of America*, 40 (2005) 1333-1341.
- [15] N.W. Schmidt, G.C.L. Wong, Antimicrobial peptides and induced membrane curvature: Geometry, coordination chemistry, and molecular engineering, *Current Opinion in Solid State and Materials Science*, 17 (2013) 151-163.
- [16] N.P. Chongsirawatana, J.S. Lin, R. Kapoor, M. Wetzler, J.A.C. Rea, M.K. Didwania, C.H. Contag, A.E. Barron, Intracellular biomass flocculation as a key mechanism of rapid bacterial killing by cationic, amphipathic antimicrobial peptides and peptoids, *Scientific Reports*, 7 (2017) 16718.

- 1 [17] E. Breukink, I. Wiedemann, C. Van Kraaij, O. Kuipers, H.-G. Sahl, B. De Kruijff,  
2 Use of the cell wall precursor lipid II by a pore-forming peptide antibiotic, *Science*,  
3 286 (1999) 2361-2364.
- 4 [18] I.J. Galván Márquez, B. McKay, A. Wong, J.J. Cheetham, C. Bean, A. Golshani,  
5 M.L. Smith, Mode of action of nisin on *Escherichia coli*, *Canadian journal of*  
6 *microbiology*, 66 (2020) 161-168.
- 7 [19] H. Rottenberg, The measurement of membrane potential and  $\Delta pH$  in cells,  
8 organelles, and vesicles, *Methods Enzymol*, 55 (1979) 547-569.
- 9 [20] A. Peña, S. Uribe, J.P. Pardo, M. Borbolla, The use of a cyanine dye in  
10 measuring membrane potential in yeast, *Archives of Biochemistry and Biophysics*,  
11 231 (1984) 217-225.
- 12 [21] A.P. Singh, P. Nicholls, Cyanine and safranin dyes as membrane potential  
13 probes in cytochrome c oxidase reconstituted proteoliposomes, *Journal of*  
14 *Biochemical and Biophysical Methods*, 11 (1985) 95-108.
- 15 [22] G. Milligan, P.G. Strange, Reduction in accumulation of  
16 [3H]triphenylmethylphosphonium cation in neuroblastoma cells caused by optical  
17 probes of membrane potential: Evidence for interactions between carbocyanine  
18 dyes and lipophilic anions, *Biochimica et Biophysica Acta (BBA) - Molecular Cell*  
19 *Research*, 762 (1983) 585-592.
- 20 [23] A.S. Waggoner, Dye Indicators of Membrane Potential, *Annual Review of*  
21 *Biophysics and Bioengineering*, 8 (1979) 47-68.
- 22 [24] G. Cabrini, A.S. Verkman, Localization of cyanine dye binding to brush-border  
23 membranes by quenching of n-(9-anthroyloxy) fatty acid probes, *Biochimica et*  
24 *biophysica acta*, 862 (1986) 285-293.
- 25 [25] P.J. Sims, A.S. Waggoner, C.-H. Wang, J.F. Hoffman, Mechanism by which  
26 cyanine dyes measure membrane potential in red blood cells and  
27 phosphatidylcholine vesicles, *Biochemistry*, 13 (1974) 3315-3330.
- 28 [26] S.J.B.j. Krasne, Interactions of voltage-sensing dyes with membranes. I.  
29 Steady-state permeability behaviors induced by cyanine dyes, 30 (1980) 415-439.
- 30 [27] S. Krasne, Interactions of voltage-sensing dyes with membranes. II.  
31 Spectrophotometric and electrical correlates of cyanine-dye adsorption to  
32 membranes, *Biophys J*, 30 (1980) 441-462.
- 33 [28] P. Breeuwer, J. Drocourt, F.M. Rombouts, T. Abee, A Novel Method for  
34 Continuous Determination of the Intracellular pH in Bacteria with the Internally  
35 Conjugated Fluorescent Probe 5 (and 6-)-Carboxyfluorescein Succinimidyl Ester,  
36 *Applied and environmental microbiology*, 62 (1996) 178-183.
- 37 [29] S.C. Kuo, J.O. Lampen, Osmotic Regulation of Invertase Formation and  
38 Secretion by Protoplasts of *Saccharomyces*, *Journal of*  
39 *Bacteriology*, 106 (1971) 183.
- 40 [30] G.Y. Lomakina, Y.A. Modestova, N.N. Ugarova, Bioluminescence assay for cell  
41 viability, *Biochemistry. Biokhimiia*, 80 (2015) 701-713.
- 42 [31] B.L. Roth, M. Poot, S.T. Yue, P.J. Millard, Bacterial viability and antibiotic  
43 susceptibility testing with SYTOX green nucleic acid stain, *Applied and*  
44 *Environmental Microbiology*, 63 (1997) 2421.

- 1 [32] M. Yasir, D. Dutta, M.D.P. Willcox, Comparative mode of action of the  
2 antimicrobial peptide melimine and its derivative Mel4 against *Pseudomonas*  
3 *aeruginosa*, *Scientific reports*, 9 (2019) 7063-7063.
- 4 [33] R. Rathinakumar, W.F. Walkenhorst, W.C. Wimley, Broad-spectrum  
5 antimicrobial peptides by rational combinatorial design and high-throughput  
6 screening: the importance of interfacial activity, *Journal of the American Chemical*  
7 *Society*, 131 (2009) 7609-7617.
- 8 [34] C. Pérez-Peinado, S.A. Dias, M.M. Domingues, A.H. Benfield, J.M. Freire, G.  
9 Rádis-Baptista, D. Gaspar, M.A.R.B. Castanho, D.J. Craik, S.T. Henriques, A.S. Veiga,  
10 D. Andreu, Mechanisms of bacterial membrane permeabilization by crotalicidin  
11 (Ctn) and its fragment Ctn(15-34), antimicrobial peptides from rattlesnake venom,  
12 *The Journal of biological chemistry*, 293 (2018) 1536-1549.
- 13 [35] A.W. Coleman, M.J. Maguire, J.R. Coleman, Mithramycin- and  
14 4'-6-diamidino-2-phenylindole (DAPI)-DNA staining for fluorescence  
15 microspectrophotometric measurement of DNA in nuclei, plastids, and virus  
16 particles, *Journal of Histochemistry & Cytochemistry*, 29 (1981) 959-968.
- 17 [36] M.L. Mangoni, N. Papo, D. Barra, M. Simmaco, A. Bozzi, A. Di Giulio, A.C.J.B.J.  
18 Rinaldi, Effects of the antimicrobial peptide temporin L on cell morphology,  
19 membrane permeability and viability of *Escherichia coli*, 380 (2004) 859-865.
- 20 [37] M. Urfer, J. Bogdanovic, F.L. Monte, K. Moehle, K. Zerbe, U. Omasits, C.H.  
21 Ahrens, G. Pessi, L. Eberl, J.A.J.J.o.B.C. Robinson, A peptidomimetic antibiotic  
22 targets outer membrane proteins and disrupts selectively the outer membrane in  
23 *Escherichia coli*, 291 (2016) 1921-1932.
- 24 [38] B. Chudzik, M. Koselski, A. Czuryło, K. Trębacz, M. Gagoś, A new look at the  
25 antibiotic amphotericin B effect on *Candida albicans* plasma membrane  
26 permeability and cell viability functions, *European Biophysics Journal*, 44 (2015)  
27 77-90.
- 28 [39] C. Chatterjee, M. Paul, L. Xie, W.A. van der Donk, Biosynthesis and Mode of  
29 Action of Lantibiotics, *Chemical Reviews*, 105 (2005) 633-684.
- 30 [40] X. Wang, Q. Gu, E. Breukink, Non-lipid II targeting lantibiotics, *Biochimica et*  
31 *Biophysica Acta (BBA) - Biomembranes*, 1862 (2020) 183244.
- 32 [41] E. Breukink, H.E. van Heusden, P.J. Vollmerhaus, E. Swiezewska, L. Brunner, S.  
33 Walker, A.J. Heck, B. de Kruijff, Lipid II is an intrinsic component of the pore  
34 induced by nisin in bacterial membranes, *J Biol Chem*, 278 (2003) 19898-19903.
- 35 [42] H.E. Hasper, B. de Kruijff, E. Breukink, Assembly and Stability of Nisin-Lipid II  
36 Pores, *Biochemistry*, 43 (2004) 11567-11575.
- 37 [43] H.E. van Heusden, B. de Kruijff, E. Breukink, Lipid II induces a transmembrane  
38 orientation of the pore-forming peptide lantibiotic nisin, *Biochemistry*, 41 (2002)  
39 12171-12178.
- 40 [44] I. Wiedemann, E. Breukink, C. van Kraaij, O.P. Kuipers, G. Bierbaum, B. de  
41 Kruijff, H.-G. Sahl, Specific binding of nisin to the peptidoglycan precursor lipid II  
42 combines pore formation and inhibition of cell wall biosynthesis for potent  
43 antibiotic activity, *Journal of Biological Chemistry*, 276 (2001) 1772-1779.

- 1 [45] J. Medeiros-Silva, S. Jekhmane, A.L. Paioni, K. Gawarecka, M. Baldus, E.  
2 Swiezewska, E. Breukink, M. Weingarth, High-resolution NMR studies of antibiotics  
3 in cellular membranes, *Nature Communications*, 9 (2018) 3963.
- 4 [46] I. Wiedemann, R. Benz, H.-G. Sahl, Lipid II-Mediated Pore Formation by the  
5 Peptide Antibiotic Nisin: a Black Lipid Membrane Study, *Journal of Bacteriology*,  
6 186 (2004) 3259.
- 7 [47] J.E. Velásquez, X. Zhang, W.A. Van Der Donk, Biosynthesis of the antimicrobial  
8 peptide epilancin 15X and its N-terminal lactate, *Chemistry & biology*, 18 (2011)  
9 857-867.
- 10 [48] M.B. Ekkelenkamp, M. Hanssen, S.-T. Danny Hsu, A. de Jong, D. Milatovic, J.  
11 Verhoef, N.A.J. van Nuland, Isolation and structural characterization of epilancin  
12 15X, a novel lantibiotic from a clinical strain of *Staphylococcus epidermidis*, *FEBS*  
13 *Letters*, 579 (2005) 1917-1922.
- 14 [49] L.L. Ling, T. Schneider, A.J. Peoples, A.L. Spoering, I. Engels, B.P. Conlon, A.  
15 Mueller, T.F. Schäberle, D.E. Hughes, S. Epstein, M. Jones, L. Lazarides, V.A.  
16 Steadman, D.R. Cohen, C.R. Felix, K.A. Fetterman, W.P. Millett, A.G. Nitti, A.M.  
17 Zullo, C. Chen, K. Lewis, A new antibiotic kills pathogens without detectable  
18 resistance, *Nature*, 517 (2015) 455-459.
- 19 [50] R. Shukla, F. Lavore, S. Maity, M.G.N. Derks, C.R. Jones, B.J.A. Vermeulen, A.  
20 Melcrová, M.A. Morris, L.M. Becker, X. Wang, R. Kumar, J. Medeiros-Silva, R.A.M.  
21 van Beekveld, A. Bonvin, J.H. Lorent, M. Lelli, J.S. Nowick, H.D. MacGillavry, A.J.  
22 Peoples, A.L. Spoering, L.L. Ling, D.E. Hughes, W.H. Roos, E. Breukink, K. Lewis, M.  
23 Weingarth, Teixobactin kills bacteria by a two-pronged attack on the cell envelope,  
24 *Nature*, 608 (2022) 390-396.
- 25 [51] R. Shukla, J. Medeiros-Silva, A. Parmar, B.J.A. Vermeulen, S. Das, A.L. Paioni, S.  
26 Jekhmane, J. Lorent, A. Bonvin, M. Baldus, M. Lelli, E.J.A. Veldhuizen, E. Breukink, I.  
27 Singh, M. Weingarth, Mode of action of teixobactins in cellular membranes, *Nat*  
28 *Commun*, 11 (2020) 2848.
- 29 [52] A. Parmar, R. Lakshminarayanan, A. Iyer, V. Mayandi, E.T. Leng Goh, D.G.  
30 Lloyd, M.L.S. Chalasani, N.K. Verma, S.H. Prior, R.W. Beuerman, A. Madder, E.J.  
31 Taylor, I. Singh, Design and Syntheses of Highly Potent Teixobactin Analogues  
32 against *Staphylococcus aureus*, Methicillin-Resistant *Staphylococcus aureus*  
33 (MRSA), and Vancomycin-Resistant Enterococci (VRE) in Vitro and in Vivo, *Journal*  
34 *of Medicinal Chemistry*, 61 (2018) 2009-2017.
- 35 [53] A.D. Paiva, E. Breukink, H.C. Mantovani, Role of lipid II and membrane  
36 thickness in the mechanism of action of the lantibiotic bovicin HC5, *Antimicrobial*  
37 *agents and chemotherapy*, 55 (2011) 5284-5293.
- 38 [54] A.J.F. Egan, R. Maya-Martinez, I. Ayala, C.M. Bougault, M. Banzhaf, E.  
39 Breukink, W. Vollmer, J.-P. Simorre, Induced conformational changes activate the  
40 peptidoglycan synthase PBP1B, *Molecular Microbiology*, 110 (2018) 335-356.
- 41 [55] H.-G. Sahl, H. Brandis, Production, purification and chemical properties of an  
42 antistaphylococcal agent produced by *Staphylococcus epidermidis*, *Microbiology*,  
43 127 (1981) 377-384.

- 1 [56] P.C. Maloney, E.R. Kashket, T.H. Wilson, A Protonmotive Force Drives ATP  
2 Synthesis in Bacteria, *Proceedings of the National Academy of Sciences*, 71 (1974)  
3 3896.
- 4 [57] R. Rashid, M. Veleba, K.A. Kline, Focal Targeting of the Bacterial Envelope by  
5 Antimicrobial Peptides, *Frontiers in cell and developmental biology*, 4 (2016) 55.
- 6 [58] L. Friedman, J.D. Alder, J.A. Silverman, Genetic changes that correlate with  
7 reduced susceptibility to daptomycin in *Staphylococcus aureus*, *Antimicrob Agents*  
8 *Chemother*, 50 (2006) 2137-2145.
- 9 [59] R. Scherrer, P. Gerhardt, Molecular sieving by the *Bacillus megaterium* cell  
10 wall and protoplast, *J Bacteriol*, 107 (1971) 718-735.
- 11 [60] L. Pasquina-Lemonche, J. Burns, R.D. Turner, S. Kumar, R. Tank, N. Mullin, J.S.  
12 Wilson, B. Chakrabarti, P.A. Bullough, S.J. Foster, J.K. Hobbs, The architecture of  
13 the Gram-positive bacterial cell wall, *Nature*, 582 (2020) 294-297.
- 14 [61] I.L. Bartek, M.J. Reichlen, R.W. Honaker, R.L. Leistikow, E.T. Clambey, M.S.  
15 Scobey, A.B. Hinds, S.E. Born, C.R. Covey, M.J. Schurr, A.J. Lenaerts, M.I. Voskuil,  
16 Antibiotic Bactericidal Activity Is Countered by Maintaining pH Homeostasis in  
17 *Mycobacterium smegmatis*, *mSphere*, 1 (2016).
- 18 [62] V.R.I. Kaila, M. Wikström, Architecture of bacterial respiratory chains, *Nature*  
19 *reviews. Microbiology*, 19 (2021) 319-330.
- 20 [63] G. Kaim, P. Dimroth, ATP synthesis by the F1Fo ATP synthase of *Escherichia*  
21 *coli* is obligatorily dependent on the electric potential, *FEBS Lett*, 434 (1998) 57-60.
- 22 [64] G. Kaim, P. Dimroth, Voltage-generated torque drives the motor of the ATP  
23 synthase, *EMBO J*, 17 (1998) 5887-5895.
- 24 [65] G. Kaim, P. Dimroth, ATP synthesis by F-type ATP synthase is obligatorily  
25 dependent on the transmembrane voltage, *EMBO J*, 18 (1999) 4118-4127.
- 26 [66] L.L. Ling, T. Schneider, A.J. Peoples, A.L. Spoering, I. Engels, B.P. Conlon, A.  
27 Mueller, T.F. Schäberle, D.E. Hughes, S. Epstein, M. Jones, L. Lazarides, V.A.  
28 Steadman, D.R. Cohen, C.R. Felix, K.A. Fetterman, W.P. Millett, A.G. Nitti, A.M.  
29 Zullo, C. Chen, K. Lewis, A new antibiotic kills pathogens without detectable  
30 resistance, *Nature*, 517 (2015) 455-459.

31

32